

# **Speed of Sound of Pure Water at Temperatures between 274 and 394 K and Pressures up to 90 MPa<sup>1</sup>**

G. Benedetto <sup>2</sup>, R. M. Gavioso <sup>2</sup>, P. A. Giuliano Albo <sup>2</sup>, S. Lago <sup>2,3</sup>, D. Madonna Ripa <sup>2</sup>  
and R. Spagnolo <sup>2</sup>

---

<sup>1</sup> Paper presented at the Fifteenth Symposium on Thermophysical Properties, June 22-27, 2003, Boulder, Colorado, U.S.A.

<sup>2</sup> Istituto Elettrotecnico Nazionale Galileo Ferraris, Strada delle Cacce 91, I-10135  
Torino, Italy

<sup>3</sup> To whom correspondence should be addressed. lago@ac.iien.it

## ABSTRACT

A newly designed experimental apparatus has been used to measure the speed of sound  $u$  in high-purity water on nine isotherms between 274 and 394 K and at pressures up to 90 MPa. The measurement technique is based on a traditional double-reflector pulse-echo method with a single piezoceramic transducer placed at unequal distances from two stainless steel reflectors. The transit times of an acoustic pulse are measured at a high sampling rate by a digital oscilloscope. The distances between the transducer and the reflectors were obtained at ambient temperature and pressure by direct measurements with a coordinate measuring machine. The speeds of sound are subject to an overall estimated uncertainty of 0.05%. The acoustic data were combined with available values of density  $\rho$  and isobaric heat capacity  $c_p$  along one isobar at atmospheric pressure, to calculate the same quantities over the whole temperature and pressure range, by means of a numerical integration technique. These results were compared with those calculated from the formulation IAPWS-95.

**KEY WORDS:** pulse-echo; pure water; speed of sound.

## 1. INTRODUCTION

Besides its basic importance in a great number of different technical and scientific applications, water is commonly used as a reference fluid for the calibration of a variety of measuring devices including experimental apparatus for the measurement of the speed of sound in liquids. As a part of an ongoing research program to develop an accurate experimental technique for the measurement of speed of sound in high pressure liquids, we considered the possibility to avoid such a calibration procedure, and obtain at the same time values of speed of sound in pure water of profitable accuracy. The speed of sound in water as a function of temperature and pressures has been extensively measured by the application of a variety of methods, nevertheless results of very high accuracy are typically available only at atmospheric pressure [1, 2], or over a limited range of temperature at higher pressures [3-5].

In this work we report measurements of speed of sound  $u$  in pure water at temperatures between 274 and 394 K and pressures up to 90 MPa. These results have been compared to those calculated from the IAPWS-95 formulation [6] and are in agreement within 0.1 % over the whole investigated temperature and pressure range.

Accurate measurements of the speed of sound in real fluids have a special interest as they offer an indirect way to obtain information on related thermodynamic properties like density and heat capacity, whose direct measurement, especially at high pressure, is extremely difficult. In order to test this possibility we combined our acoustic data with values of density  $\rho$  and isobaric specific heat capacity  $c_p$  calculated from [6] on one isobar at 0.1 MPa and, by means of the integration technique described below, determined the same quantities over the entire  $P$ - $T$  region investigated by this study.

## 2. EXPERIMENTAL

The design of the present ultrasonic apparatus is based on the double reflector pulse-echo technique [7, 8] and has been chosen in reason of its good combination of design simplicity and high achievable resolution and accuracy.

## 2.1. Ultrasonic cell

A diagram of the ultrasonic cell is shown in Fig. 1 . It is made of a hollow AISI 303 stainless steel cylinder (77 mm long, o.d. 43 mm, i.d. 33 mm) in which the ultrasonic transducer, a piezoelectric ( $\text{PbZrTiO}_3$  – Channel Industries mod. C5400) disk (diam. 10 mm, thickness 0.5 mm), is clamped at its edges between a conical support and a conical teflon insulated stainless steel ring. The conical shape of the ring and the support minimizes the interfering effect of diverging components of the acoustic beam which may be reflected on the transducer. The ring and the support are fixed to each other by means of three screws electrically insulated by small teflon collars. Two solid stainless steel reflectors (thickness 15 mm) having plane smooth surfaces, are fixed to the bases of the cell respectively at a distance of 30.5 and 46 mm. The outer surfaces of the reflectors were cut with a series of pyramid-shaped incisions in order to maximize dispersion of sound passing through the reflectors thus avoiding its back-reflection into the cell.

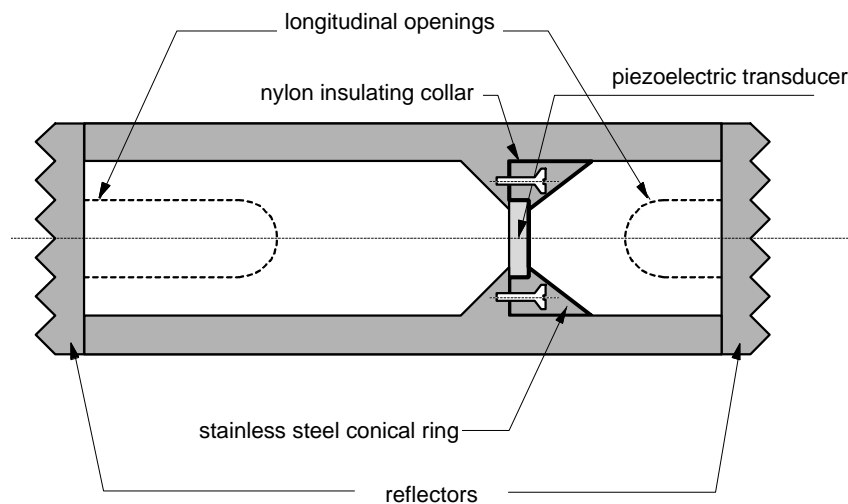


**Fig. 1.** Ultrasonic cell for measurement of speed of sound in high pressure liquids

## 2.2. Measurement of propagation time

Ultrasonic sound speed measurement basically consists in the determination of two mechanical quantities: a geometric acoustic path and the associated time interval. According to the double reflector pulse-echo technique, a function generator (Agilent 33250A) excites a piezo-ceramic transducer with an electrical signal in the form of ten-cycle repeated tone bursts with a carrier frequency of about 5 MHz and an amplitude of 10 V<sub>p-p</sub>. The transducer emits two acoustic pulses spreading simultaneously in opposite directions. Each acoustic wave train, hitting the reflector, produces a set of echoes. The electrical signal delivered to the transducer and the echoes from the reflectors are recorded by a digital oscilloscope (LeCroy LT372). The burst period is chosen low enough to obtain the complete decay of the echoes before the triggering of the next electrical pulse. The complete waveform corresponds to a duration of 100 μs and is

digitized at a sampling rate of  $4 \cdot 10^9$  samples per second. The digital signal  $P_1(t_i)$  representing the first sampled echo coming from the nearest reflector is correlated to the first echo  $P_2(t_j)$  from the farthest reflector by means of a temporal correlation function  $C(\mathbf{t})$

$$C(\mathbf{t}) = \int_{-\infty}^{+\infty} P_1(t) P_2(t + \mathbf{t}) dt, \quad (1)$$

where  $\mathbf{t} \in ]-\infty, +\infty[$  is a point in the delay time domain. A fast and reliable method to accomplish this calculation is based on the FFT algorithm and the properties of Fourier Transforms: applying the Fourier operator  $F[\dots]$  to both sides of eq. (1)

$$F[C] = F[P_1]^* F[P_2], \quad (2)$$

the correlation function is obtained at the cost of two FFT transforms and a final inverse transform on  $F[C]$ . The delay time between the two echo waveforms  $P_1(t_i)$  and  $P_2(t_j)$  is assumed as the value  $\mathbf{t}_{\text{exp}}$  which maximizes the function  $C(\mathbf{t})$ . This method has the advantage of being insensitive to amplitude differences between the two echo waveforms. The performance of the algorithm has been tested against synthetic data and found to be very robust: the addition of gaussian noise with an amplitude equal to the 10% of the maximum signal produced a difference of only one sampling interval in the determination of delay time.

Since the sound speed of interest is associated to the idealised condition of perfectly plane waves travelling in free-space, the measured transit time difference  $\mathbf{t}_{\text{exp}}$  has to be corrected for diffraction effects. Diffraction causes the wave fronts produced by a finite dimension source to lay on curved surfaces and consequently a phase shift  $\mathbf{f}(L)$  relative to a plane wave travelling the same distance [9]. The measured transit time difference  $\mathbf{t}_{\text{exp}}$  must then be increased by  $\mathbf{dt}$

$$\mathbf{dt} = \frac{\mathbf{f}(2L_2) - \mathbf{f}(2L_1)}{\mathbf{w}_0}, \quad (3)$$

$$\mathbf{f}(L) = \text{Arg} \left( 1 - \frac{4}{\mathbf{p}} \int_0^{\mathbf{p}/2} \exp \left[ -i \left( \frac{2\mathbf{w}_0 b^2}{uL} \right) \cos^2 \mathbf{J} \right] \text{sen}^2 \mathbf{J} d\mathbf{J} \right), \quad (4)$$

where  $\mathbf{w}_0$  is the angular frequency of the carrier,  $u$  the sound speed,  $L_1$  and  $L_2$  the distance between the source and the reflectors,  $b$  the source radius. The measured speed of sound is obtained from  $u_{\text{meas}} = \frac{2\Delta L(T, P)}{\mathbf{t}_{\text{corr}}}$ , where  $\Delta L = L_2 - L_1$  and  $\mathbf{t}_{\text{corr}} = \mathbf{t}_{\text{exp}} + \mathbf{dt}$ .

Considering the mutual dependence of  $\mathbf{dt}$  and  $u_{\text{meas}}$ , their values are found by iteration. The diffraction correction for our experimental apparatus amounted to less than 0.015% of the measured transit time difference.

## 2.2. Dimensional Measurements

A coordinate measuring machine was used to determine the difference  $\Delta L$  between the length of the acoustic paths  $L_1$  and  $L_2$ .

The machine had a resolution and a repeatability of 0.1  $\mu\text{m}$  and an accuracy of approximately 1  $\mu\text{m}$ . Measurements were carried out in a thermostatted room at ambient pressure  $P_0$ . Five successive measuring sequences were accomplished, each one consisting of nine randomly spaced points on the two surfaces of the PZT transducer and the flat faces of the cell sidewall. The maximum difference between the five evaluations of  $L_{1,2}$  was less than 1  $\mu\text{m}$ . Though it is likely that the major unknown systematic uncertainty components associated to the coordinates measurement would cancel out in the difference operation, we associated the uncertainty of  $\pm 2 \mu\text{m}$  to the determined values  $L_1 = 30.592$  and  $L_2 = 45.997$ . Finally the determined difference in the acoustic path was  $\mathbf{DL} = 15.405 \pm 0.004$  mm. The variation of  $\mathbf{DL}$  with temperature and pressure was calculated as  $\mathbf{DL}(T,P) = \mathbf{DL}(T_0, P_0)(1 + \mathbf{a}DT + \mathbf{b}DP)$  where  $\mathbf{a}$  and  $\mathbf{b}$  are respectively the coefficients of thermal expansion [9] and the coefficient of compressibility of 303 stainless steel; the latter was calculated from the values of the elastic constants of the same material. The magnitude of the corrections required for the path length were 0.034% at the maximum pressure (90 MPa) and temperature (394 K).

## 2.3. High-pressure system

The high-pressure system consists of three main sections: the pressure vessel, a pressure monitoring and measuring line and a pressure control device. The vessel and the measuring line can be completely isolated from the other parts of the system in order to minimize heat exchange effects on the thermostatted vessel. Pressure is generated and controlled by a 100 MPa pressure amplifier connected to a low pressure liquid reservoir which contains the sample under test. A pressure transducer (SENSOTEC TJE/4843-01 TJA) was used to measure the pressure in the system with an uncertainty of 0.04 MPa as estimated from the calibration between 20 and 90 MPa against a pressure balance (national standard). The pressure vessel, specifically designed for this application, is made from a stainless steel alloy and has an internal volume of 420  $\text{cm}^3$ . It is provided with two coaxial pressure-tight electrical feedthrough for high frequency signals transmission from the ambient to the ultrasonic cell and can be operated with pressures up to 100 MPa and in a temperature range of 230 K - 400 K.

## 2.4. Temperature measurement and control

The ultrasonic cell and the pressure vessel were placed in a stirred liquid bath thermostat based on a Dewar vessel with a capacity of approximately 60  $\text{dm}^3$ . Heat losses through the wall and the lid of the vessel were further reduced with a 7 cm thick polystyrene insulating coating. The fluid within the bath was a silicone oil (Dow Corning 200/100cs). Temperature was maintained and controlled by a system consisting of a main thermostat (Julabo FP50) having a stability of  $\pm 0.01$  mK, and a proportional-integral-derivative controller operating with a platinum resistance probe and a 60 W

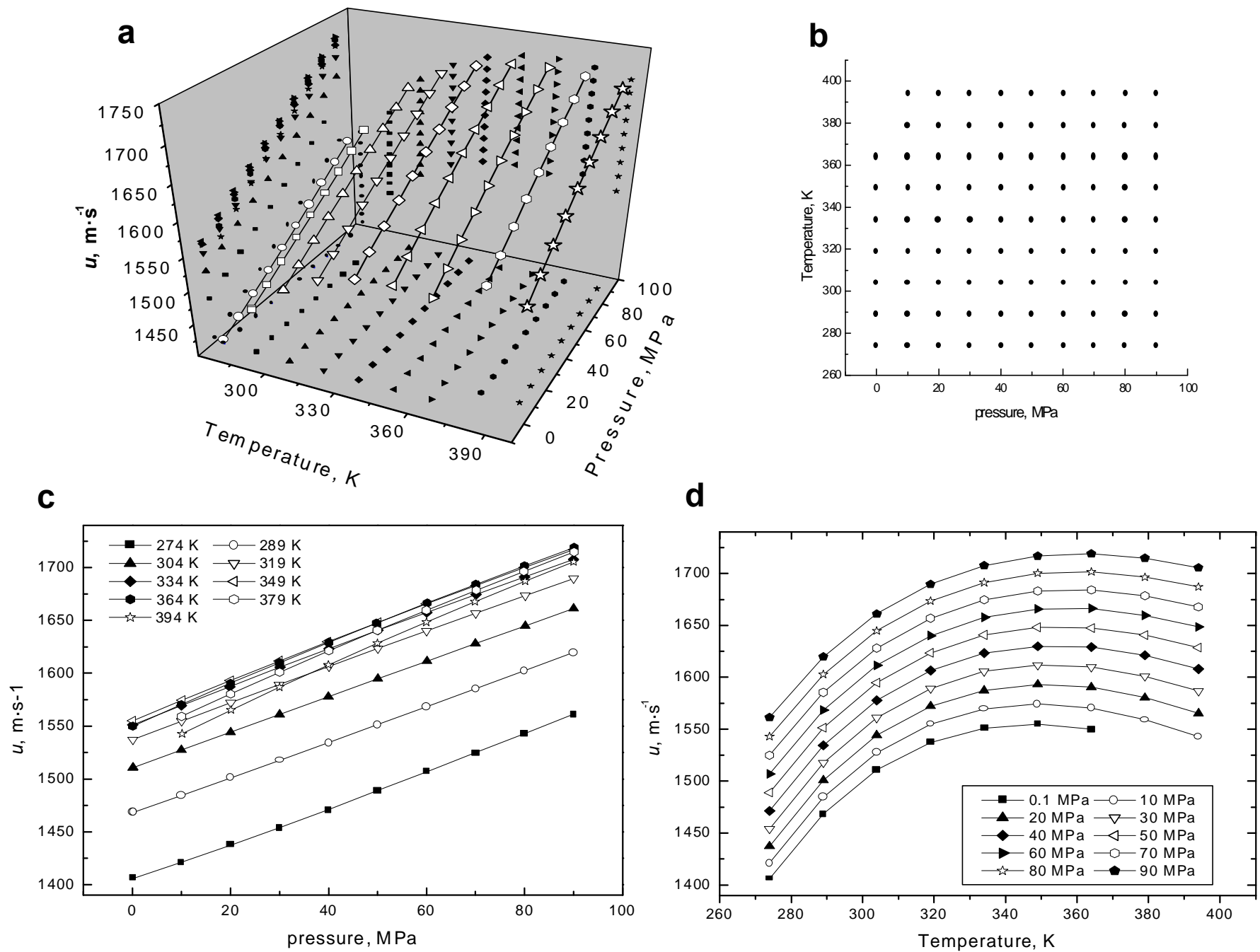


**Fig. 2.** Speed of sound of water: a) as function of pressure and temperature; b)  $P$ - $T$  investigated region; c) isotherms as a function of pressure; d) isobars as a function of temperature

incandescence bulb which served for the control heater. This system permitted to achieve a long-term temperature stability within the bath of  $\pm 2$  mK over the whole operating temperature range. The temperature associated to speed of sound measurements was determined with an accuracy of  $\pm 0.01$  K as the average of the readings of two platinum resistance thermometers (PRTs), calibrated by comparison with a standard PRT, which were attached to the top and bottom parts of the pressure vessel. The temperature gradient recorded by the two PRTs in the course of the present speed of sound measurements, was within 10 mK, with the exception of the lowest isotherm at 274 K; in this case the top of the vessel was 20 mK warmer than the bottom suggesting that a thermal link from the top to ambient temperature existed.

## 2.5. Purity of water sample

The deionized water sample used in this study had a specified minimum purity of 99.99% by volume. It has been obtained by means of an active resins filtering device (Millipore) with a stated electrolytic conductivity of  $0.054 \mu\text{S}\cdot\text{cm}^{-1}$  and a concentration of particles ( $0.22 \mu\text{m}$ )  $< 1/\text{ml}$ , however it is likely that this extremely high level of deionization and purity of the water sample was substantially lowered as it came in contact with the different metal parts composing the experimental apparatus. The ultrasonic cell was filled under vacuum.

## 3. RESULTS

### 3.1. Speed of sound in water. Results and comparison with IAPWS-95

The experimental values of the speed of sound  $u$  in water at 90 points are listed in Table I. and represented in Fig. 2 as a function of temperature and pressure.

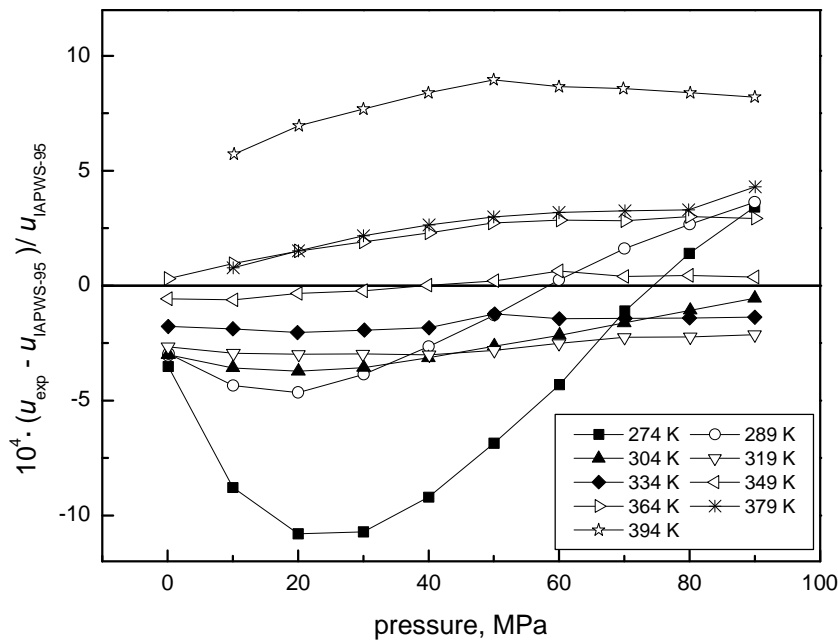


**Fig. 3.** Deviations of experimental speed of sound from IAPWS-95 formulation

**Table I.** Experimental values of speed of sound in water

$p$ (MPa)	$u$ (m·s <sup>-1</sup> )	$p$ (MPa)	$u$ (m·s <sup>-1</sup> )	$p$ (MPa)	$u$ (m·s <sup>-1</sup> )	$p$ (MPa)	$u$ (m·s <sup>-1</sup> )	$p$ (MPa)	$u$ (m·s <sup>-1</sup> )
$T = 273.98$ K									
0.09	1406.04	20.00	1437.35	40.03	1471.26	60.05	1506.71	79.96	1543.00
10.00	1421.25	30.01	1454.05	50.04	1488.84	70.09	1524.95	89.94	1561.31
$T = 289.01$ K									
0.09	1468.43	20.02	1500.96	40.02	1534.46	59.97	1568.35	80.03	1602.59
0.17	1468.57	30.04	1517.68	50.05	1551.44	70.04	1585.53	90.00	1619.64
10.04	1484.56								
$T = 303.99$ K									
0.10	1510.61	20.05	1544.26	39.98	1577.80	60.06	1611.42	80.11	1644.77
0.18	1510.76	30.05	1561.11	50.06	1594.71	70.00	1627.98	90.01	1661.14
10.02	1527.37								
$T = 319.00$ K									
0.09	1537.16	20.10	1572.22	40.09	1606.52	59.99	1640.14	80.10	1673.45
10.07	1554.73	29.95	1589.20	50.07	1623.46	70.01	1656.84	90.00	1689.64
$T = 334.00$ K									
0.09	1551.17	19.90	1587.38	40.07	1623.16	60.02	1657.59	79.99	1691.11
10.00	1569.43	30.13	1605.65	50.11	1640.66	70.10	1674.60	90.00	1707.59
$T = 349.00$ K									
0.09	1554.92	20.00	1593.14	39.89	1629.85	60.00	1665.68	79.99	1700.01
10.17	1574.45	30.00	1611.76	50.12	1648.22	70.07	1683.08	90.02	1716.83
$T = 364.00$ K									
0.09	1549.99	20.02	1590.45	40.04	1629.15	60.15	1666.36	79.99	1701.58
9.99	1570.35	30.01	1609.99	49.77	1647.37	70.06	1684.09	90.09	1719.00
$T = 379.00$ K									
10.05	1559.21	30.01	1600.94	50.00	1640.57	70.12	1678.50	90.06	1714.66
20.06	1580.44	40.06	1621.12	59.97	1659.60	79.88	1696.31		
$T = 394.00$ K									
10.16	1542.62	30.01	1586.75	49.98	1628.50	69.89	1667.71	90.02	1705.48
20.15	1565.19	39.96	1607.85	59.97	1648.41	80.10	1687.10		

These measurements were carried out on nine isotherms between 274 and 394 K, in approximately 10 MPa pressure decrements from 90 MPa to atmospheric pressure, with the exception of the isotherms at 379 K and 394K where low pressure readings were limited to a minimum of 10 MPa, due to the sample being in the vapor state at atmospheric pressure. Since an adiabatic decrease in pressure of 10 MPa sensibly changed the temperature inside the pressure vessel and the ultrasonic cell, it was necessary to wait approximately 1 h until, according to the indications of the two thermometers attached to the pressure vessel, thermal equilibrium was reestablished and a new measurement was made.

Figure 2c shows intersecting isotherms; this is to be expected since  $u$  decreases at low pressure for temperatures higher than  $\sim 347.2$  K [10]. The characteristic shift of the speed of sound maximum towards higher temperatures as a function of increasing pressure can be observed in Fig. 2d.

We have compared our results to the predictions of the formulation of the International Association for the Properties of Water and Steam (IAPWS-95) [6]. The estimated uncertainty of the formulation in speed of sound ranges from  $\pm 0.005\%$  at atmospheric pressure to a maximum of  $\pm 0.1\%$  over the  $P$ - $T$  region interested by our measurements. As represented in Fig. 3 most of our results show deviations from IAPWS-95 which are within 0.05%, with the exception of the lowest and highest temperature isotherms at 274 K and 394 K whose deviations are within 0.1%. The smoothness and low scatter of the deviations as evident on the scale of Fig. 3 show the satisfactory level of precision achieved with the present experimental apparatus and measurement procedures.

### 3.2 Estimation of the measurement uncertainty

From a metrological point of view, the pulse-echo technique for sound speed determination is an indirect measurement method described by the following model

$$u_{meas} = \frac{2\Delta L}{t} = u(\Delta L, t, T, P), \quad (5)$$

where  $\Delta L$  and  $t$  are independent mechanical determinations and  $P, T$  are parameters. Consequently, standard equations for error propagation can be applied, giving:

$$\frac{s(u_{meas})}{u_{meas}} = \sqrt{\left(\frac{s(\Delta L)}{\Delta L}\right)^2 + \left(\frac{s(t)}{t}\right)^2 + \left(\frac{T}{u_{meas}} \frac{\partial u_{meas}}{\partial T}\right)^2 \left(\frac{s(T)}{T}\right)^2 + \left(\frac{P}{u_{meas}} \frac{\partial u_{meas}}{\partial P}\right)^2 \left(\frac{s(P)}{P}\right)^2}. \quad (6)$$

Table II lists the major components of the standard uncertainty from the measurement of the quantities in eq. (6). Evaluating the uncertainty related to the determination of the acoustic path lengths, we do not take account of the contribution of  $\mathbf{a}$  and  $\mathbf{b}$  parameters which appear in the correction formula discussed in Sec 2.2. The uncertainty associated to time delay measurements is prudently assumed to be equal to 0.5 ns, corresponding to two oscilloscope sampling intervals; however, the high signal-to-noise ratio in the resulting waveforms and the very good resolution of the pulse correlation technique could further reduce this estimate. Temperature measurements are assumed to be

affected by an uncertainty of 0.01 K, corresponding to the calibration accuracy. Uncertainty in the determination of thermodynamic sound speed depends on an incorrect association of the measured values to the actual thermodynamic  $P$ - $T$  state of the sample. In this framework, our pressure measurement plays a major role in the magnitude of the overall uncertainty, due to the poor accuracy (0.04 MPa) of the pressure transducer in the low pressure region (0.1 MPa – 10 MPa) of the experimental plan. The estimated relative uncertainty, considered to be representative over the entire pressure range, has been calculated by a weighted mean; the sensibility factors  $\left(\frac{T}{u_{meas}} \frac{\partial u_{meas}}{\partial T}\right)$  and  $\left(\frac{P}{u_{meas}} \frac{\partial u_{meas}}{\partial P}\right)$  which appear in eq. (6) have been derived from the experimental sound speeds by means of a polynomial interpolating function.

**Table II.** Uncertainty budget

Uncertainty Source		Relative Magnitude
Determination of the acoustic	$\mathbf{s}(\Delta L)/\Delta L$	0.026 %
Determination of Temporal Delay	$\mathbf{s}(t)/t$	0.002 %
Temperature Measurements	$\left(\frac{\partial u}{\partial T}\right) \frac{\mathbf{s}(T)}{u}$	0.003 %
Pressure Measurements	$\left(\frac{\partial u}{\partial P}\right) \frac{\mathbf{s}(P)}{u}$	0.03 %
Estimated Overall Uncertainty		0.05 %

Finally, the relative uncertainty in sound speed values is estimated to be 0.05% over the entire  $P$ - $T$  region examined.

### 3.2. Derivation of density and isobaric specific heat capacity

From the experimentally determined sound speed data points, it is possible to work out the density function  $\mathbf{r}(T, P)$ , i. e. the equation of state of the fluid under test, and the isobaric specific heat capacity function  $c_p(T, P)$  over the  $P$ - $T$  region examined, given a set of independent  $\mathbf{r}$  and  $c_p$  determinations on a single (but otherwise arbitrary) isobar. The starting relations are

$$\left(\frac{\partial \mathbf{r}}{\partial P}\right)_T = \frac{T \mathbf{a}_P^2}{c_p} + \frac{1}{u^2}, \quad (7)$$

$$\left(\frac{\partial c_p}{\partial P}\right)_T = -\frac{T}{\mathbf{r}} \left[ \mathbf{a}_P^2 + \left(\frac{\partial \mathbf{a}_P}{\partial T}\right)_P \right], \quad (8)$$

$$\mathbf{a}_P = -\frac{1}{\mathbf{r}} \left(\frac{\partial \mathbf{r}}{\partial T}\right)_P, \quad (9)$$

where  $\mathbf{a}_P$  is the thermal expansion coefficient and  $u$  the sound speed. Given a suitable initial condition, in the form of  $\mathbf{r}(T, P_0)$  and  $C_p(T, P_0)$  functions at the starting pressure  $P_0$ , equations (7 - 9) form a complete first order differential equations system that can be integrated over the entire pressure range covered by the  $u(T, P)$  function.

We used a Cash-Karp, adaptive step size Runge-Kutta method which provides a fifth order approximation to differential systems. Raw sound speed experimental data have been interpolated by means of the Akima algorithm [11], a locally bivariate quintic polynomial generator, in order to produce an orthogonal mesh of sound speed values in the  $P$ - $T$  space. The system of eqs. (7-9) was then been integrated over the entire pressure and temperature range, using a B-SPLINE sixth order interpolating function to calculate the derivatives which appear in eqs. (7-9). The integration program proceeded along nine isothermal lines starting from atmospheric pressure, apart from the last two isotherms (379 K and 394 K), which start from 10.0 MPa.

The integration procedure was first tested on synthetic data drawn from the IAPWS-95 formulation and found to reproduce densities values with a maximum relative deviation of 1 ppm. The corresponding agreement for isobaric heat capacities was within  $2 \cdot 10^{-4}$  with the only exception of the lower isotherm at 274 K, whose maximum deviation from reference values was  $2 \cdot 10^{-3}$ . We consider this problem to be the result of the inaccurate evaluation of derivatives that appear in the right side of eq. (8) for points on the boundary of the integration region, as pointed out in [5].

A comparison between density data, calculated with the procedure discussed above from our experimental values of sound speed, and the reference values from IAPWS-95 is shown in Fig. 4a; it can be noted an overall good agreement, apart from the above mentioned anomaly at 274 K (the declared relative uncertainty for IAPWS-95 density data is  $\pm 10^{-5}$ ). In Fig. 4b, the results of an analogous comparison for the calculated isobaric heat capacities is shown; the anomalous 274 K isotherm has been eliminated to enhance graphical rendering. Apparently the greater deviations for the isotherm at 394 K are determined by the corresponding greater sound speed deviations from reference values which directly influence the algorithmic reconstruction of the  $c_p(T, P)$  function.

## 5. CONCLUSIONS

Speed of sound measurements on samples of purified water in an extended region of  $P$ - $T$  space have been used to test a newly assembled ultrasonic apparatus against available data. The results and the uncertainty evaluation demonstrate a quite good performance of the whole measurement system and suggest further improvements: a better precision and accuracy in the thermodynamic point determination (the uncertainty budget reported in Tab. II, evidences the role of pressure sensors as precision-limiting

devices) and an improved piezo-clamping mechanism to guarantee a higher degree of parallelism between the ultrasonic source and reflectors, reducing the uncertainty in acoustic paths evaluation.

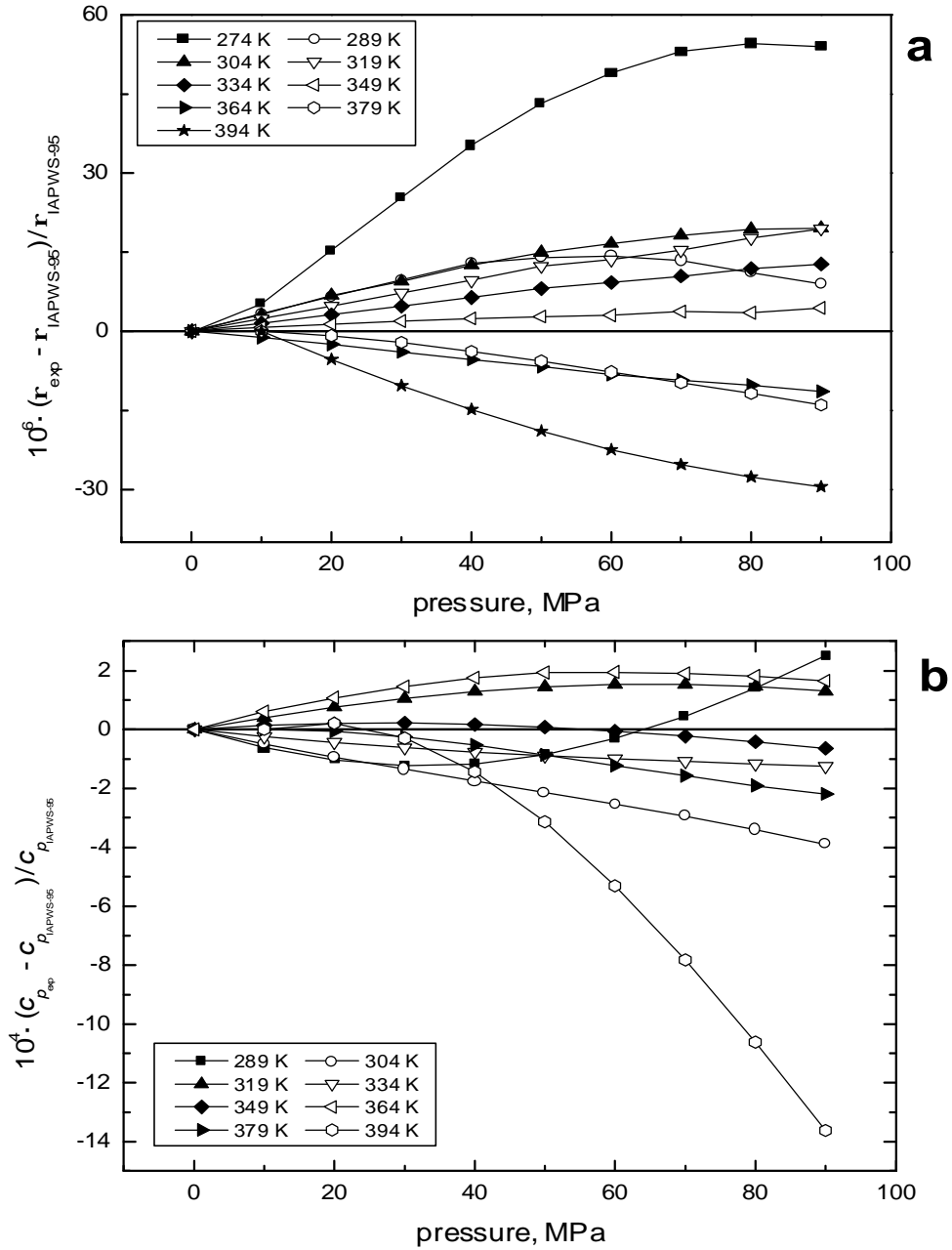


**Fig. 4.** a) Deviations of calculated densities of water from IAPWS-95 formulation;  
b) Deviations of calculated isobaric heat capacities of water from IAPWS-95 formulation.

## REFERENCES

1. V. A. Del Grosso and C. W. Mader, *J. Acoust. Soc. Am.* **52**:1442 (1972).
2. K. Fujii and R. Masui, *J. Acoust. Soc. Am.* **93**:276 (1993).
3. K. Fujii, paper presented at the 13<sup>th</sup> Symposium on Thermophysical Properties, Boulder Colorado, USA (1997).
4. A. A. Alexandrov and A. I. Kochetov, *Therm. Eng.* **26**:558 (1979).
5. J. P. Petitet, R. Tufeu and B. La Neindre, *Int. J. Thermophys.* **4**:35 (1983).
6. W. Wagner and A. Pruss, *J. Phys. Chem. Ref. Data* **31**:387 (2002).
7. P.J. Kortbeek, M.J.P. Muringer, N.J. Trappeniers, S.N. Biswas, *Rev. Sci. Instrum.*, **56**:1269, (1985).
8. S. J. Ball and J.P.M. Trusler, *Int. J. Thermophys.* **22**:427 (2001).
9. ASM Committee on wrought stainless steels, in *Metals Handbook*, (9<sup>th</sup> ed., American Society for Metals, 1980)
10. W. D. Wilson, *J. Acoust. Soc. Am.*, **31**:1067 (1959).
11. H. Akima, *ACM Trans. Math. Softw.*, **4**:148 (1978).